

Supporting Information

Evaluating cellular uptake efficiency of nanoparticles investigated by three-dimensional imaging

Yeongchang Goh^a, Yo Han Song^a, Gibok Lee^a, Hyeongyu Bae^a, Manoj Kumar Mahata^a, and

Kang Taek Lee^{a,*}

^a Department of Chemistry, Gwangju Institute of Science and Technology, 123
Cheomdangwagi-ro, Buk-gu, Gwangju, 61005, Korea

* Corresponding author: ktlee@gist.ac.kr

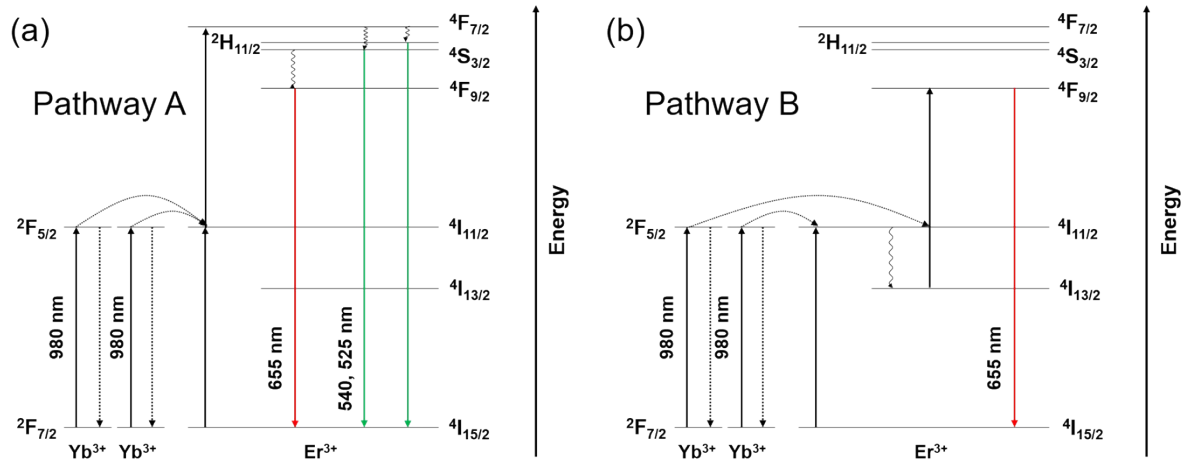


Fig. S1 Energy level diagrams of lanthanide-doped upconversion nanoparticles (UCNPs, β - $\text{NaYF}_4:\text{Yb}^{3+},\text{Er}^{3+}/\text{NaYF}_4$). (a) The green bands (525 and 540 nm), and a small fraction of red band (655 nm) are produced by pathway A. (b) The primary red band (655 nm) is produced by pathway B.

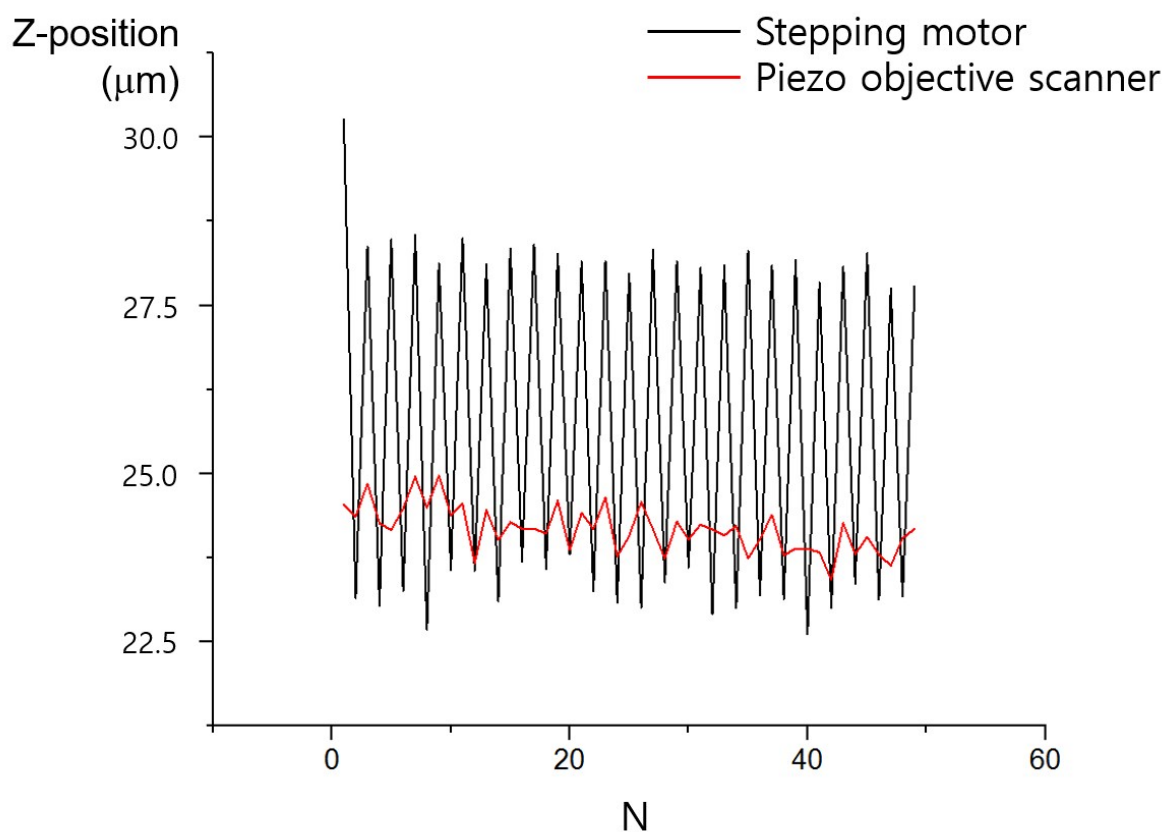


Fig. S2 The accuracy measurements of the stepping motor (black) and piezo (red) objective scanner for a fixed UCNP on fast scanning. N means repetition number of scanning. For the stepping motor, the average position was 25.7936 μm and the standard deviation was 0.2578 μm . For the piezo objective scanner, the average position was 24.176 μm and standard deviation was 0.0343 μm .

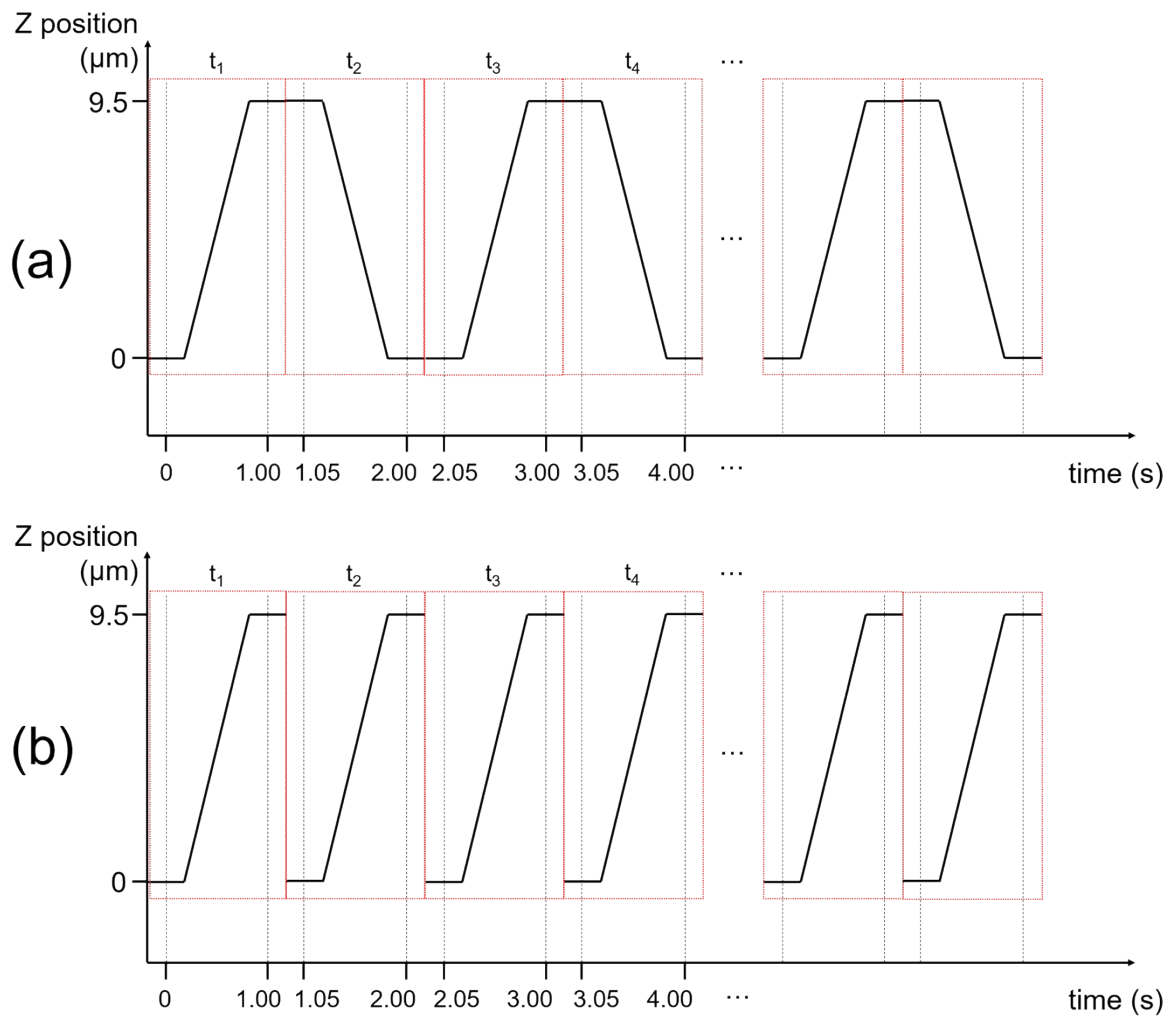


Fig. S3 Movement of the piezo objective scanner. (a) The actual upward (odd-numbered t_1, t_3, \dots) and downward (even-numbered t_2, t_4, \dots) scanning profile (b) Scanning directions of even-numbered data are reversed in order to analyze the data with consistent direction.

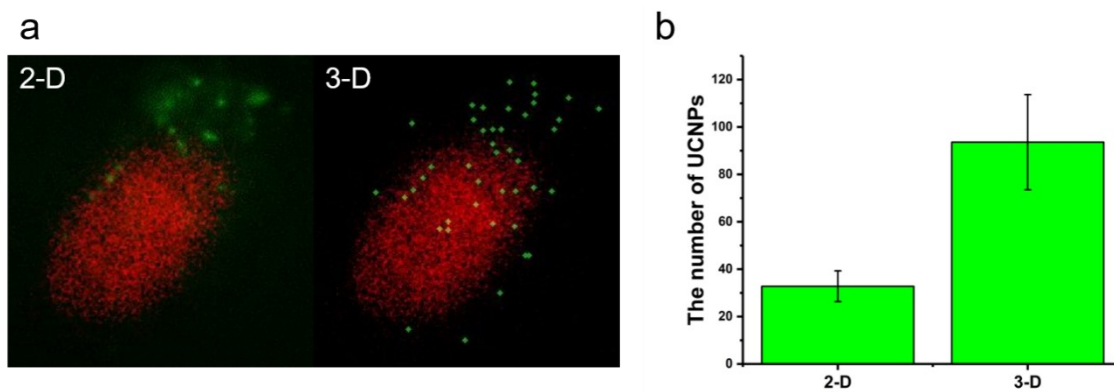


Fig. S4 The comparison of the UCNPs' number in 2-D and 3-D images for UCNP-TAT. (a) Images showing UCNPs (green) and the nucleus (red) in 2-D and 3-D. (b) Histograms showing the comparative number of UCNPs in 2-D and 3-D. The number of UCNPs were 33 ± 7 and 94 ± 20 in 2-D and 3-D, respectively.

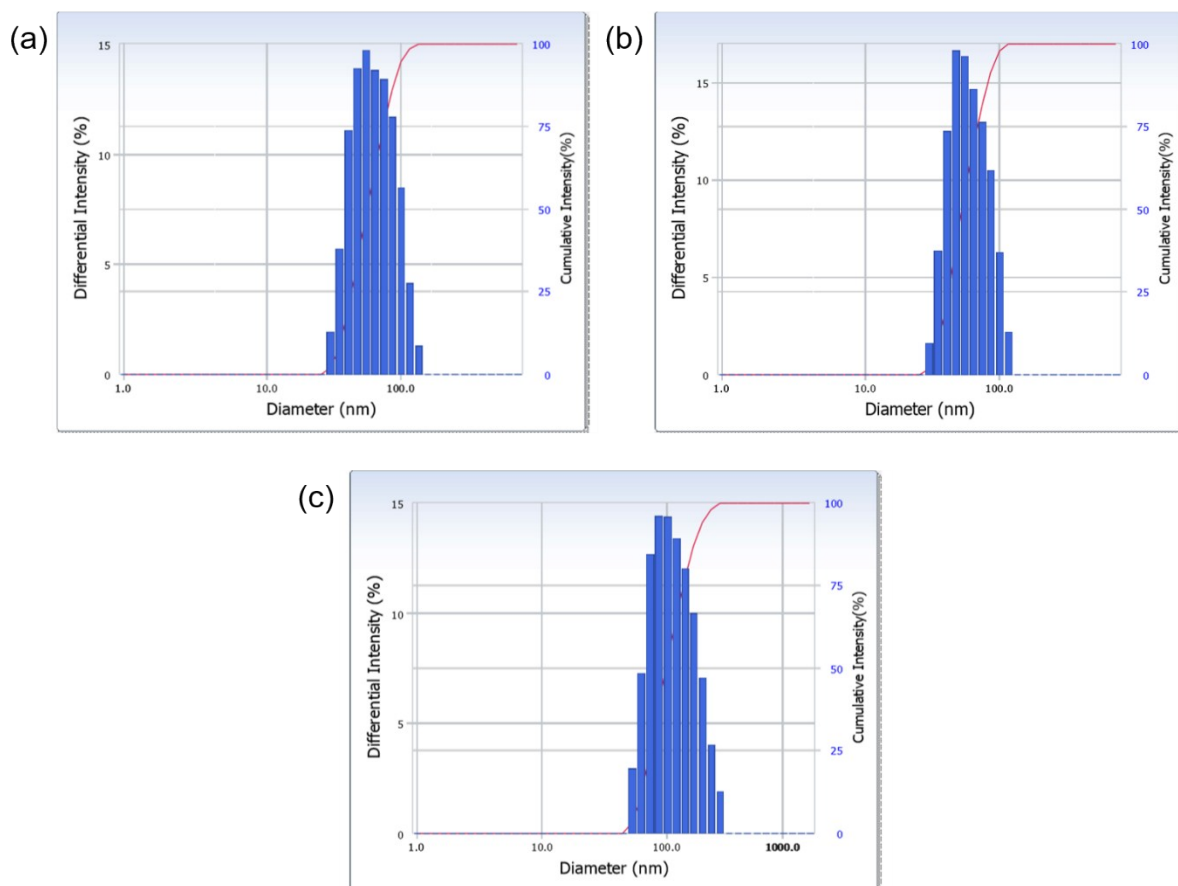


Fig. S5 Dynamic light scattering (DLS) size distribution histograms of (a) UCNP-COO⁻, (b) UCNP-NH₃⁺, and (c) UCNP-TATs. The hydrodynamic diameters are 59.3 nm, 58.3 nm, and 117.9 nm, respectively.

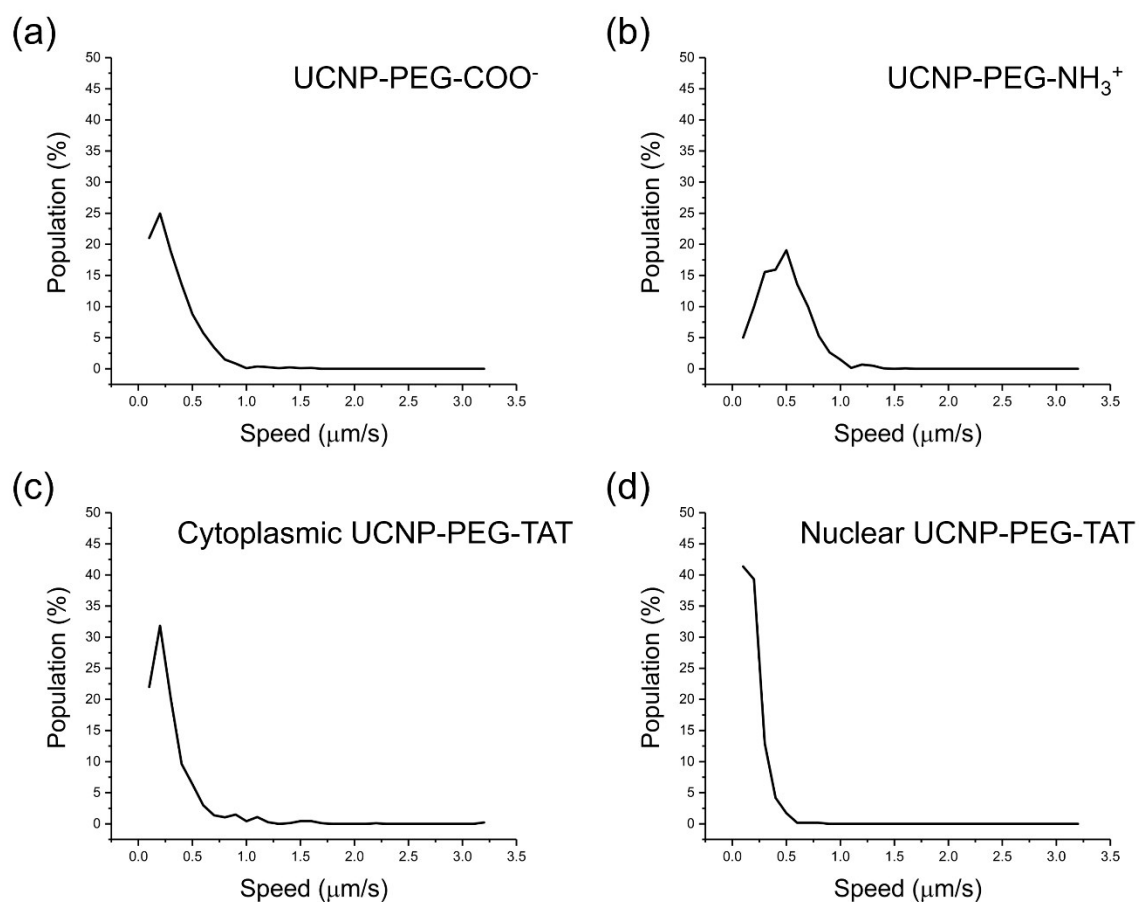


Fig. S6 The speed distributions of (a) UCNP-phospholipid-PEG-COO⁻, (b) UCNP-phospholipid-PEG-NH₃⁺, (c) UCNP-phospholipid-PEG-TAT in cytoplasm, and (d) UCNP-phospholipid-PEG-TAT in nuclei.

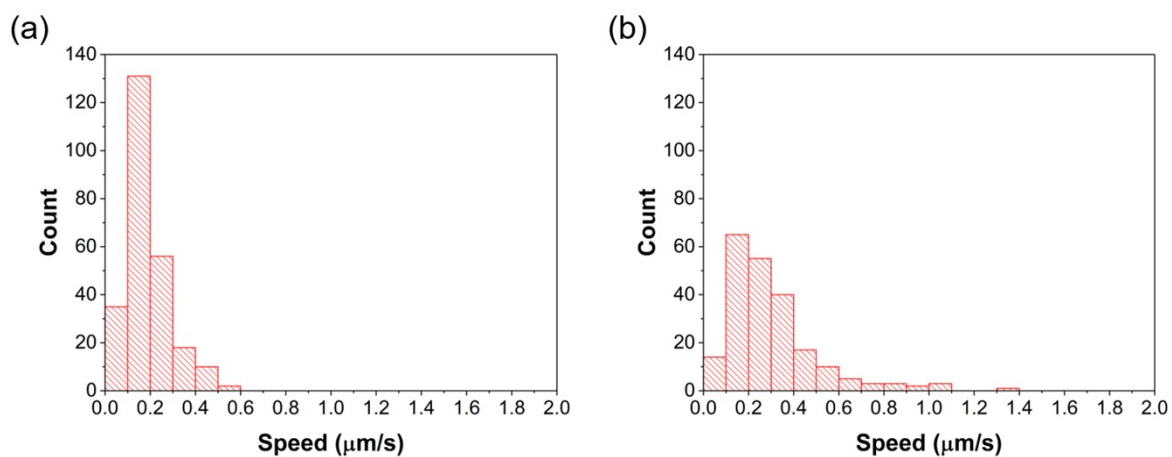


Fig. S7 The speed distribution histograms of (a) UCNP-TATs near the nuclei, and (b) UCNP-TATs in cytoplasm. The speed values of UCNP-TATs near the nuclei have maximum of 0.6 μm/s, but, the speed values of UCNP-TATs in cytoplasm have more than 0.6 μm/s.

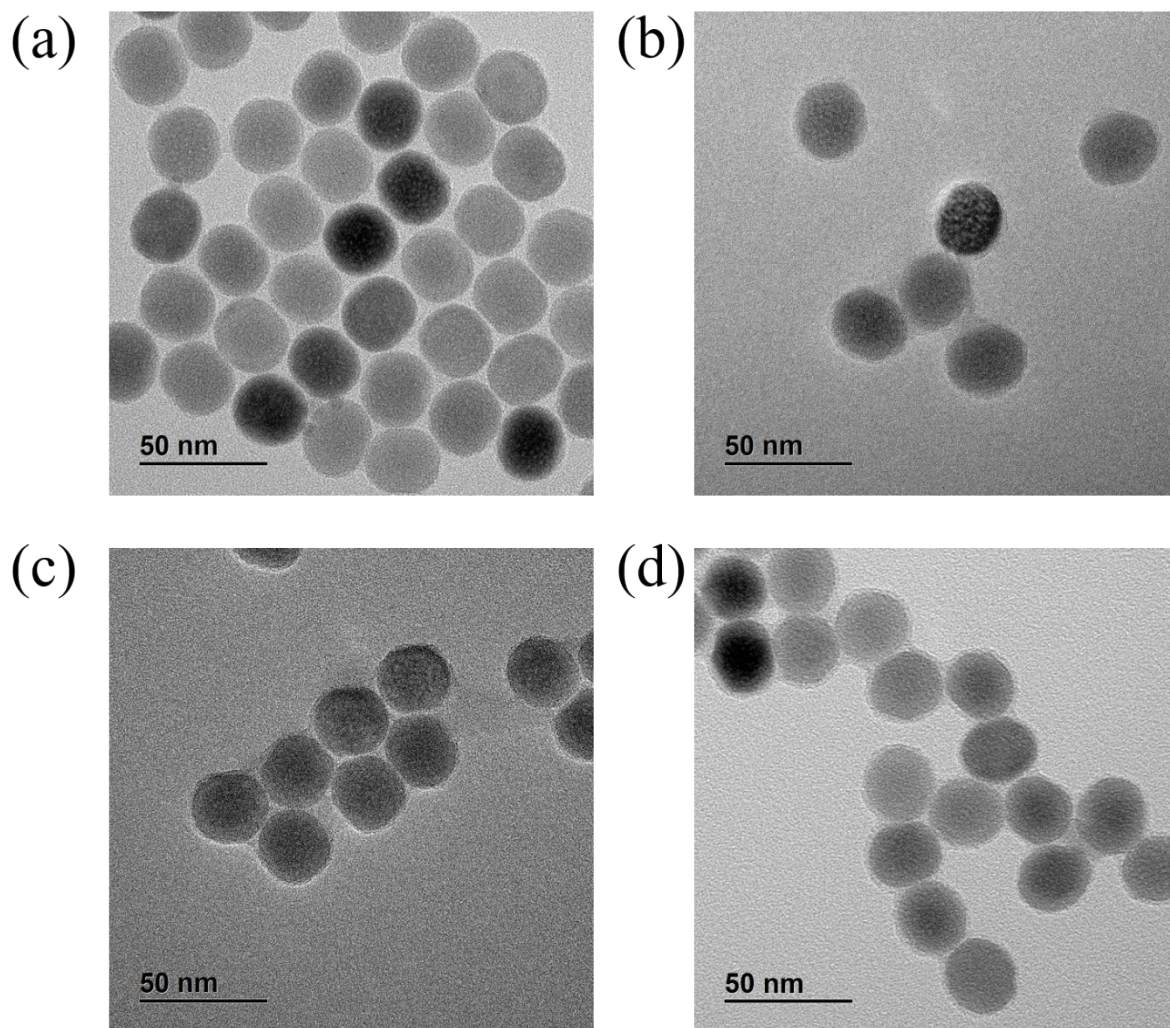


Fig. S8 TEM images of (a) core/shell UCNPs (β -NaYF₄:Yb³⁺, Er³⁺/NaYF₄), (b) carboxylic acid-functionalized-UCNPs, (c) amine-functionalized UCNPs and (d) TAT peptide conjugated UCNPs.

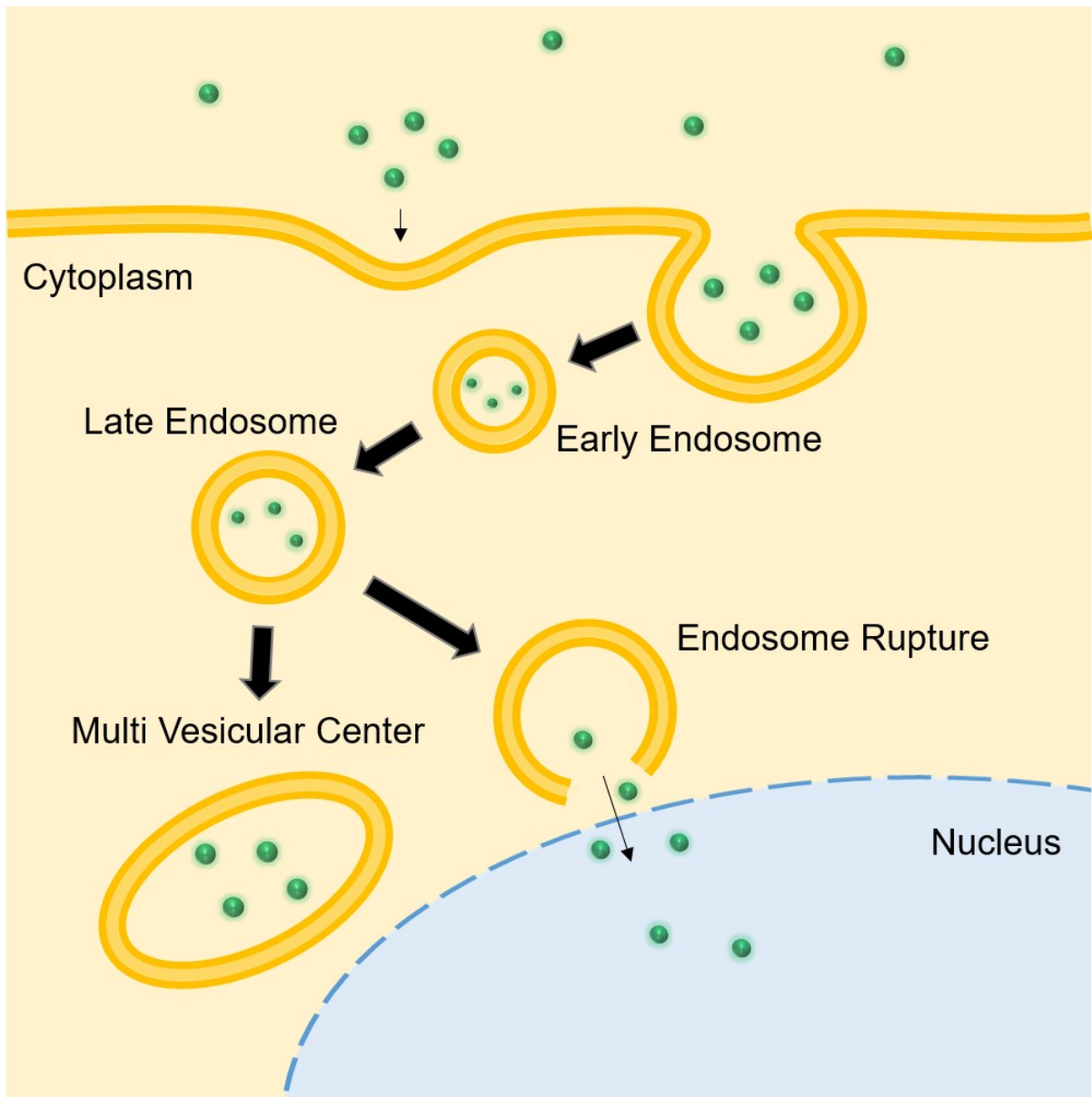


Fig. S9 The scheme of uptake pathway of UCNPs. After endocytosis, late endosome forms multi-vesicular bodies or endosome rupture. UCNPs conjugated with TAT peptide can enter the nucleus through nuclear pores.

Table S1 The statistical significance by Kruskal-wallis statistics: UCNPs ($K = 26.456$, $p = 0.000$, $p < 0.05$) Means with the same letter are not significantly different ($p > 0.05$), Duncan post hoc grouping : $a > b > c > d$

Group	Counts (n=5)
UCNP-COO⁻	59 (± 5)
UCNP-NH₃⁺	35 (± 10)
UCNP-TATs	94 (± 20)
UCNP-COO⁻ (24h of incubation)	7 (± 5)
UCNP-NH₃⁺ (24h of incubation)	9 (± 2)
UCNP-TATs (24h of incubation)	95 (± 18)